Bioconjugate Chemistry

Article

pubs.acs.org/bc

Intracellular Delivery of Antisense Peptide Nucleic Acid by Fluorescent Mesoporous Silica Nanoparticles

Xing Ma,[†,‡] Gitali Devi,[†] Qiuyu Qu,[†] Desiree-Faye Kaixin Toh,[†] Gang Chen,*[,†] and Yanli Zhao*[,†,‡]

[†]Division of Chemistry and Biological Chemistry, School of Physical and Mathematical Sciences, Nanyang Technological University, 21 Nanyang Link, 637371, Singapore

[‡]School of Materials Science and Engineering, Nanyang Technological University, 639798, Singapore

Supporting Information

ABSTRACT: In order to overcome poor cell permeability of antisense peptide nucleic acid (PNA), a fluorescent mesoporous silica nanoparticle (MSNP) carrier was developed to successfully deliver antisense PNA into cancer cells for effective silence of B-cell lymphoma 2 (Bcl-2) protein expression *in vitro*. First, fluorescent MSNP functionalized with disulfide bond bridged groups was fabricated and characterized. Antisense and negative control PNAs were synthesized and further conjugated with fluorescent dye cyanine 5. Then, the PNAs were covalently connected with fluorescent MSNP via amidation between amino group of PNAs and carboxylic acid group on the MSNP surface. High intracellular concentration of glutathione serves as a natural reducing agent, which could cleave the disulfide bond to trigger the PNA release *in vitro*. Confocal laser scanning microscopy studies prove that PNA conjugated MSNP was endocytosed by HeLa cancer cells, and redox-controlled intracellular release of antisense PNA from fluorescent MSNP was successfully achieved. Finally, effective silencing of the Bcl-2 protein expression induced by the delivered antisense PNA into HeLa cells was confirmed by Western blot assay.

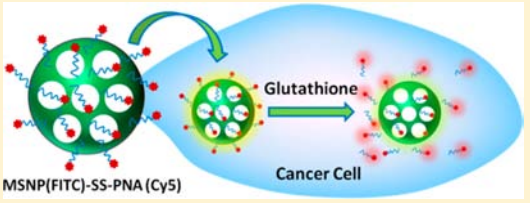

INTRODUCTION

The pro- and anti-apoptotic species in the B-cell lymphoma 2 (Bcl-2) protein family maintain a balance for cell proliferation and death.[1,2] In certain cases, overexpression of anti-apoptotic Bcl-2 protein leads to the prevention of cell death and thus the resistance of chemotherapy and radiotherapy. The silencing of Bcl-2 protein has been employed to enhance traditional chemotherapy efficacy.[3−5] Peptide nucleic acid (PNA) is a mimic of DNA and RNA, with repeating *N*-(2-aminoethyl)-glycine units and the nucleobases connected to the backbone via a methylene carbonyl linker.[6,7] Compared to DNA and RNA, PNA has greater binding affinity toward complementary DNA and RNA, partially because of its flexible and neutral backbone. Earlier reports have suggested that the use of antisense PNA in micromolar to nanomolar concentrations can effectively and selectively silence gene expression.[8−11] Importantly, the efficiency of down-regulation is determined by the internalization of PNA into cells. However, a major disadvantage that limits the antisense application of PNA is its poor cell permeability. In order to overcome this drawback, substantial work has been carried out to achieve intracellular PNA delivery.[12] For example, covalent conjugation of PNA to cell-penetrating peptides and lipids for intracellular PNA delivery was reported.[8,10,11] Gold nanoparticles and dendrimers as carriers were also utilized for the PNA delivery.[13,14]

As an excellent intracellular delivery vehicle, mesoporous silica nanoparticles (MSNP) have been utilized for nucleic acid delivery.[15,16] Conventional nucleic acid delivery was based on electrostatic interactions between positively charged nanoparticle surface and negatively charged nucleic acid. Such a method is not applicable for delivering essentially neutral PNA into cells in a controlled release manner. To the best of our knowledge, there has been so far no report on using MSNP to controllably deliver PNA into cells for gene silencing.

Herein, we report MSNP-based PNA delivery system that can effectively deliver an antisense PNA sequence into cancer cells for efficient silencing of Bcl-2 protein expression (Scheme 1). PNA was covalently conjugated onto MSNP through a disulfide linkage. The disulfide bond embedded on the MSNP surface is redox-responsive, and thus intracellular glutathione (GSH) could trigger the disulfide bond cleavage[17−19] for facilitating the release of PNA inside cancer cells. It is challenging to controllably release the nucleic acids after intracellular uptake in electrostatic interaction-based nucleic acid delivery methods. In the present MSNP-based PNA delivery system, redox-triggered cleavage of the disulfide linkage inside cells can ensure effective PNA release after intracellular uptake. The PNA sequence complementary to the first six codons of open reading frame of Bcl-2 mRNA,[11,20] denoted as PNA(Bcl-2), was chosen for this work. PNA(Bcl-2) with and without cyanine 5 (Cy5) fluorescent labeling dye (Table 1) were covalently conjugated onto fluorescein isothiocyanate (FITC) labeled MSNP (MSNP(FITC)), denoted as MSNP-(FITC)-SS-PNA(Cy5) and MSNP(FITC)-SS-PNA(Bcl-2),

Received: October 26, 2013
Revised: July 21, 2014
Published: July 23, 2014

Scheme 1. Illustration of the PNA Conjugation with FITC Labeled MSNP and Redox-Triggered Intracellular Release of Cy5 Labeled PNA

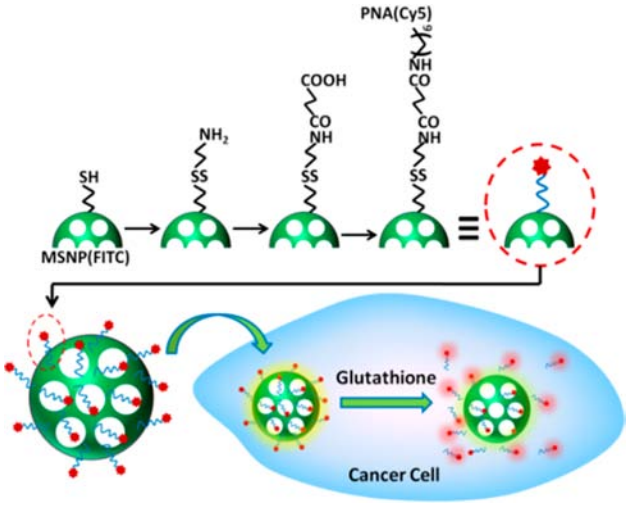

respectively. Experimental results indicate that, compared to free PNA(Cy5), MSNP(FITC)-SS-PNA(Cy5) shows increased cellular internalization without any significant cytotoxicity, and the antisense PNA released from MSNP(FITC)-SS-PNA(Bcl-2) could bind to complementary mRNA in cytoplasm to silence the expression of Bcl-2 protein inside cancer cells.

RESULTS AND DISCUSSION

MSNP(FITC) was prepared by a co-condensation method according to a previously reported procedure.[17,21] Thiol group was grafted on the surface of MSNP(FITC). Then, surfactant cetyltrimethylammonium bromide (CTAB) was removed by refluxing MSNP(FITC)-SH in acidic methanol overnight. As a control, amino group-containing MSNP(FITC) without disulfide bond (MSNP(FITC)-NH_2) was prepared by refluxing MSNP(FITC) with 3-aminopropyltriethoxysilane in ethanol. MSNP(FITC)-SH and MSNP(FITC)-NH_2 were characterized by powder X-ray diffraction (XRD) and N_2 adsorption/desorption measurements. In the XRD patterns (Figure S1a in the Supporting Information (SI)), the characteristic (001) peak at 2θ = 2.3° for both MSNP(FITC)-SH and MSNP(FITC)-NH_2 reveals a hexagonally packed structure of MCM-41 type mesoporous silica. Typical type IV isotherms further support their mesoporous nature (Figure S1b in the SI). Specific Brunauer−Emmett−Teller (BET) surface areas were found to be 790.06 $m^2\ g^{-1}$ for MSNP(FITC)-SH and 797.38 $m^2\ g^{-1}$ for MSNP(FITC)-NH_2 (Table S1 in the SI).

After reacting MSNP(FITC)-SH with *S*-(2-aminoethylthio)-2-thiopyridine hydrochloride, the disulfide bond-containing nanoparticles were obtained, denoted as MSNP(FITC)-SS-NH_2. Then, the amino groups on MSNP(FITC)-NH_2 and MSNP(FITC)-SS-NH_2 were treated with succinic anhydride, leading to carboxylic acid-containing nanoparticles MSNP-(FITC)-COOH and MSNP(FITC)-SS-COOH, respectively. The formed nanoparticles, MSNP(FITC)-SS-COOH, were characterized by field emission scanning electron microscopy (FE-SEM) and transmission electron microscopy (TEM). The mesoporous nanoparticles with a uniform size distribution of 110 nm in diameter were observed (Figure 1a,b, and Figure S2 in the SI).

The functionalization process was traced by Fourier transformed infrared (FT-IR) spectrometer (Figure 2) and zeta potential measurements (Table S2 in the SI). The grafting of thiol groups was evidenced by a minor peak at 2560 cm^{-1} in the FT-IR spectrum of MSNP(FITC)-SH. After the formation of a disulfide bond, a new peak at 1520 cm^{-1} due to primary amino group was observed in the FT-IR spectrum of MSNP(FITC)-SS-NH_2. When MSNP(FITC)-SS-NH_2 was converted to MSNP(FITC)-SS-COOH, the peaks at 1720 cm^{-1} from −COOH and 1560 cm^{-1} from −NH− in the amide bond were found. The conjugation of PNAs was also clearly indicated by the FT-IR spectrum of MSNP(FITC)-SS-PNA-(Cy5). Due to a large amount of amino groups and amide bonds in MSNP(FITC)-SS-PNA(Cy5), obvious peaks at 3300 and 3086 cm^{-1} were observed. In addition, the peak intensities at 1650 and 1543 cm^{-1} were enhanced in the case of MSNP(FITC)-SS-PNA(Cy5). After the disulfide bond formation, zeta potential value of the nanoparticles changed from −33.6 mV (MSNP(FITC)-SH) to 32.5 mV (MSNP(FITC)-SS-NH_2). Further converting −NH_2 to −COOH resulted in a strong negative zeta potential value of −42.2 mV for MSNP(FITC)-SS-COOH. The PNA conjugation greatly decreased the surface charge from −42.2 mV to −9.10 mV for MSNP(FITC)-SS-PNA(Cy5). Similar evolution was observed in both FT-IR spectra and zeta potential measurement for the preparation of nanoparticles without disulfide bond (MSNP(FITC)-PNA(Cy5), Figure S3 and Table S2 in the SI), indicating successful functionalization.

Functional MSNP was expected to have higher PNA delivery capacity than solid nanoparticle based delivery system. In order to prove this hypothesis, we prepared solid SiO_2 with a similar nanoparticle size using a modified Stöber method[22] (Figure S4 in the SI), followed by the same surface functionalization. Then, the surface functional group of −SS-NH_2 was quantified by the fluorescamine method in methanol solution (see detailed procedure in the Experimental Section). As expected, significantly higher density of the functional groups on MSNP-SS-NH_2 (233.9 ± 24.0 nmol mg^{-1}) than solid SiO_2-SS-NH_2 (7.0 ± 1.1 nmol mg^{-1}) was observed (Figures S5 and S6 in the SI). The porous nature of MSNP in a nanoscale size could show much higher surface area for the grafting of functional groups. Under the same mass, MSNP would give a larger number of nanoparticles than that of solid SiO_2. Thus, higher efficiency of PNA conjugation onto the MSNP surface than solid SiO_2 nanoparticles under the same conditions was achieved.

Table 1. PNA Oligomers Synthesized for This Work

PNAs	sequence (from N−C terminus)	molecular formula	calculated molecular weight	observed molecular weight
PNA(Bcl-2)	TCTCCCAGCGTGCGCCAT (antisense)	$C_{195}H_{246}N_{100}O_{57}$	4901.94	4903.76
PNA(Cy5)	TCTCCCAGCGTGCGCCAT-Cy5	$C_{230}H_{291}N_{106}O_{58}$	5467.31	5468.16
PNA(−)	TGTGTTGCGACCCTCTTG (nonsense)	$C_{198}H_{249}N_{97}O_{61}$	4960.93	4962.08
PNA(Bcl-2 mm)	TCTCCCATCGTTCGCCAT (mismatch)	$C_{195}H_{248}N_{94}O_{59}$	4852.65	4853.81

dx.doi.org/10.1021/bc5002714 | *Bioconjugate Chem.* 2014, 25, 1412−1420

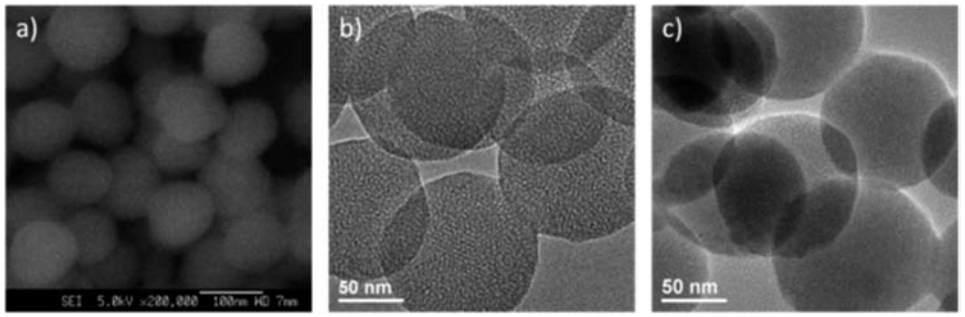

Figure 1. (a) FE-SEM image of MSNP(FITC)-SS-COOH. TEM images of (b) MSNP(FITC)-SS-COOH and (c) MSNP(FITC)-SS-PNA(Cy5).

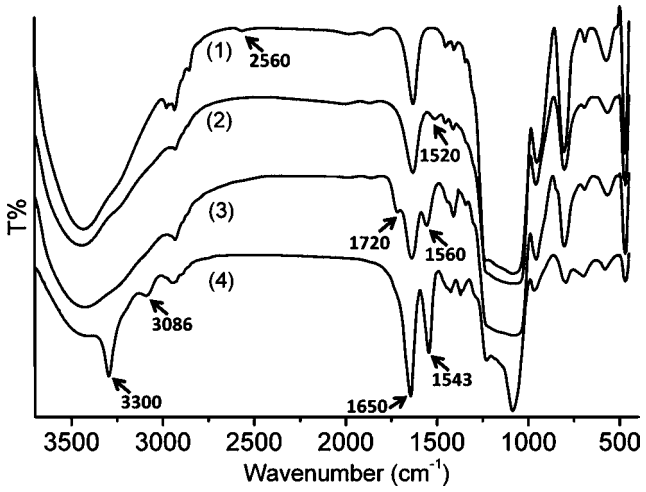

Figure 2. FT-IR spectra of various MSNPs. (1) MSNP(FITC)-SH, (2) MSNP(FITC)-SS-NH_2, (3) MSNP(FITC)-SS-COOH, and (4) MSNP(FITC)-SS-PNA(Cy5).

PNAs used for this work were prepared by the solid phase peptide synthesis method (see Experimental Section). All PNAs were purified by reverse phase high-performance liquid chromatography (RP-HPLC, Figure S7 in the SI) and characterized by matrix-assisted laser desorption/ionization-time-of-flight mass spectrometry (MALDI-TOF MS, Figure S8 in the SI). The alkyne functionality at the *C*-terminus of 18-mer antisense PNA(Bcl-2) was introduced by using a propargyl glycine unit. To introduce fluorescent PNA(Cy5), alkyne functionalized PNA was reacted with azide-containing Cy5 fluorescent dye via copper-catalyzed click chemistry.[23] An arbitrary PNA sequence PNA(−), of which basic local alignment search tool (BLAST) database shows no homology with any known mammalian gene or DNA sequence,[24] was prepared as a negative control. PNA(Cy5), PNA(Bcl-2), PNA(−), and a PNA with double mutation (PNA(Bcl-2 mm), Table 1) were then covalently conjugated onto the MSNP(FITC) surface through the amide bond formation. The amidation between primary amino group at the *N*-terminus of PNA and carboxylic acid group on MSNP(FITC)-SS-COOH or MSNP(FITC)-COOH was carried out to afford the MSNP-PNA conjugates with or without the disulfide bonds (MSNP-(FITC)-SS-PNA(Cy5) or MSNP(FITC)-PNA(Cy5)). To ensure complete removal of unreacted PNAs after the conjugation, the nanoparticles were washed thoroughly with deionized water. A successful conjugation of PNA(Cy5) onto MSNP(FITC) was indicated by the presence of absorbance maxima at 485 and 650 nm in the UV−vis spectra, corresponding to FITC and Cy5 units, respectively (Figure 3a). After the PNA conjugation, the size of the nanoparticles did not change obviously, but the mesoporous structure was obscured on account of the PNA coverage on the nanoparticle surface (Figure 1c).[21] Fluorescent emission spectra (Figure 3b) of FITC and Cy5 units in the MSNP-PNA conjugates were well separated, and no obvious emission from Cy5 (or FITC) was observed when only FITC (or Cy5) was excited. Such fluorescence emission independence is useful for monitoring intracellular PNA(Cy5) release by detecting these two different emissions.

Redox-triggered PNA(Cy5) release from MSNP(FITC)-SS-PNA(Cy5) was first investigated by using reducing agent dithiothreitol (DTT) in PBS buffer at pH 7.2 (Figure 4). Upon addition of 10 mM DTT, continuous PNA(Cy5) release was

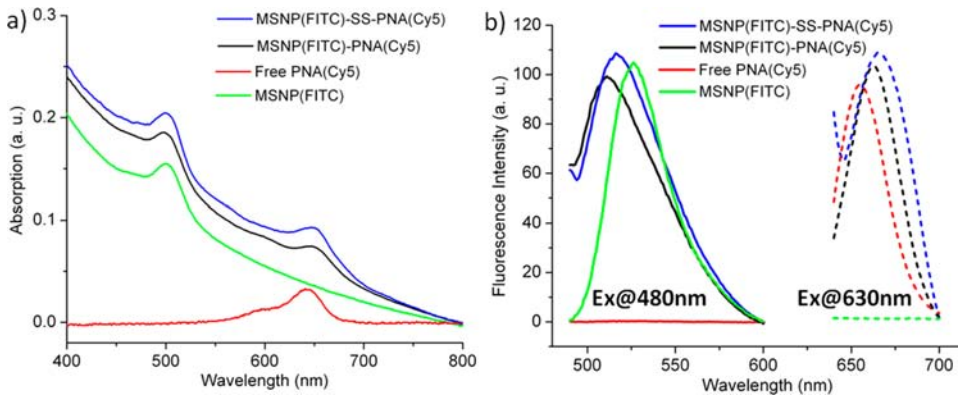

Figure 3. (a) UV−vis absorption and (b) fluorescence emission spectra of MSNP(FITC)-SS-PNA(Cy5), MSNP(FITC)-PNA(Cy5), free PNA(Cy5), and MSNP(FITC). For the fluorescence emission, the solid curves were excited at 480 nm, and dashed curves were excited at 630 nm.

dx.doi.org/10.1021/bc5002714 | *Bioconjugate Chem.* 2014, 25, 1412−1420

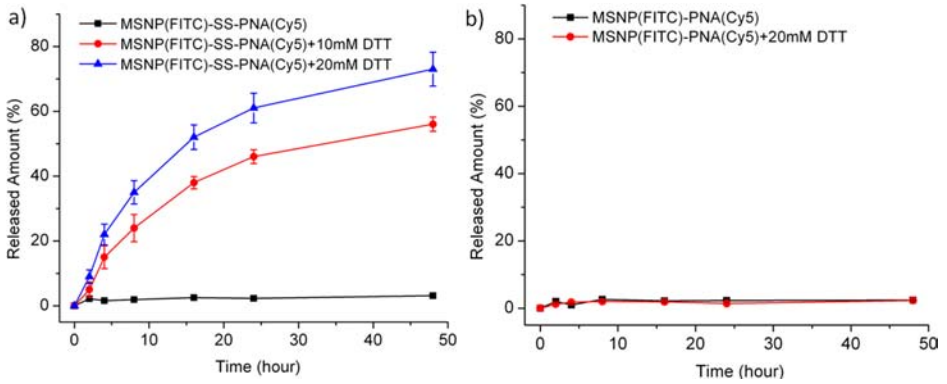

Figure 4. PNA(Cy5) release profiles from (a) MSNP(FITC)-SS-PNA(Cy5) and (b) MSNP(FITC)-PNA(Cy5) in PBS buffer (pH 7.2) with or without the DTT addition.

observed. Higher DTT concentration (20 mM) led to quicker release rate, further proving the redox-controlled release property. Without the addition of any reducing agent, no PNA(Cy5) was released, even after incubation for 2 days, as indicated by the black curve (Figure 4a). As a control, we also investigated the release behavior of MSNP(FITC)-PNA(Cy5) without the disulfide bond. After the addition of 20 mM DTT, there was no PNA(Cy5) release from MSNP(FITC)-PNA-(Cy5), further confirming the disulfide bond cleavage controlled PNA(Cy5) release. Moreover, the conjugated PNA(Cy5) amount on the nanoparticles was determined to be about 5 wt %, by comparing the fluorescence intensity of the supernatant of MSNP(FITC)-SS-PNA(Cy5) after adding excess DTT to release all PNA(Cy5) with a standard sample.

The release process of nucleic acids from the nanoparticle carriers after endocytosis was barely mentioned in the literature. Thus, we investigated intracellular release of PNA(Cy5) in HeLa cell line by observing the fluorescence emissions of MSNP(FITC) and PNA(Cy5). HeLa cells were first treated with MSNP(FITC)-SS-PNA(Cy5) (20 μg mL^{-1}, corresponding to ~0.2 μM PNA(Cy5)) for a series of time intervals. Before monitoring by confocal laser scanning microscopy (CLSM), the cells were washed by PBS buffer (pH 7.2) three times to remove any nanoparticles not taken by the cells. The cell nucleus was stained by 4′,6-diamidino-2-phenylindole (DAPI) that emits blue color when excited by 405 nm laser. Initially, the red fluorescence from Cy5 completely overlapped with green color from FITC to produce a yellow color in the merged image, indicating that PNA(Cy5) was still covalently conjugated with MSNP(FITC) (Figure 5). With increasing time, red fluorescent dots that did not overlap with the green dots were observed in the cytoplasm of HeLa cells, demonstrating the PNA(Cy5) release. The disulfide bond connecting PNA(Cy5) and MSNP(FITC) could be cleaved inside HeLa cells by natural reducing agent, i.e., GSH, which facilitated the PNA(Cy5) release inside the cytoplasm. As expected, the area and intensity of red fluorescence color outside the overlaid yellow dots kept increasing from 8 to 24 h, while the yellow dots remained after 24 h, suggesting that PNA(Cy5) was not completely released from the MSNP(FITC) carrier, probably due to decreased GSH concentration in the cytoplasm.[25]

On the other hand, in the absence of the disulfide bond, PNA(Cy5) cannot be released from MSNP(FITC)-PNA(Cy5), since all the green fluorescence dots (Figure S9a in the SI) still overlapped well with red fluorescence dots (Figure S9b in the

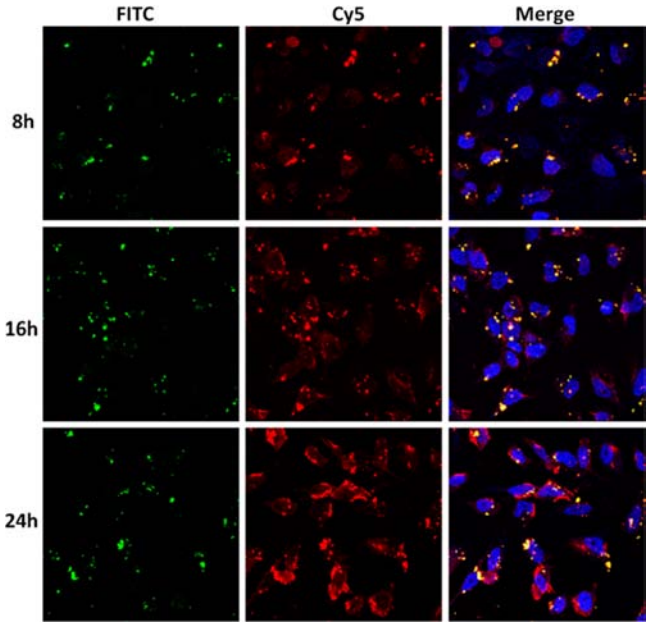

Figure 5. Monitoring of intracellular PNA(Cy5) release from MSNP(FITC)-SS-PNA(Cy5) by time-dependent CLSM taken from HeLa cells. Figures from left to right are FITC, Cy5, and merged channels, respectively.

SI) to yield yellow colored dots in the overlay image (Figure S9c in the SI). In order to better demonstrate the overlapping, an enlarged image from Figure S9c was presented as Figure S9d, from which we cannot find extra red color in the cytoplasm, unlike the case of MSNP(FITC)-SS-PNA(Cy5) (Figure 5). Low cellular uptake was observed by using free PNA(Cy5) at high concentration (1 μM, Figure S10 in the SI), indicating the good efficacy of the PNA delivery into the cytoplasm of HeLa cells by the MSNP(FITC) carrier with cleavable disulfide bond linkage.

Encouraged by the successful delivery of PNA into HeLa cells, we moved forward to investigate the efficacy of protein silencing by delivering antisense PNA against Bcl-2 gene, i.e., PNA(Bcl-2) from MSNP(FITC)-SS-PNA(Bcl-2). Here, β-actin protein was used as an internal standard for the quantification of the Bcl-2 protein expression. As shown in the Western blot assay (Figure 6), upon increasing the concentration of MSNP(FITC)-SS-PNA(Bcl-2), the intensity of the Bcl-2 protein band decreased, indicating successful silencing of Bcl-2 protein expression by the released PNA(Bcl-2) sequence.

dx.doi.org/10.1021/bc5002714 | *Bioconjugate Chem.* 2014, 25, 1412−1420

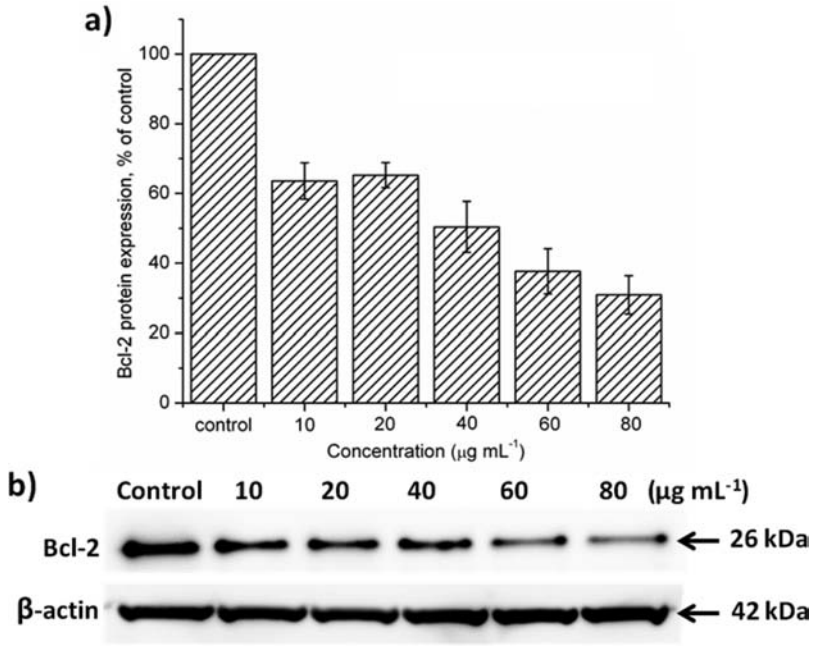

Figure 6. (a) Relative Bcl-2 protein expression levels and (b) Western blot data of HeLa cells treated with MSNP(FITC)-SS-PNA(Bcl-2) at various concentrations. The relative protein expression levels were semiquantified by comparing the Bcl-2 band intensity to the β-actin band intensity. HeLa cells without any treatment were used as control.

When the concentration of MSNP(FITC)-SS-PNA(Bcl-2) increased to 80 μg mL^{-1}, relative Bcl-2 protein expression level decreased to 30% as referred to the control (Figure 6). Compared to previously established PNA delivery strategies, the present method based on the MSNP carrier shows effective protein silence capability with the utilization of small amount of PNA.[10−14,26] There was no obvious silencing effect observed for HeLa cells treated with the negative control, i.e., MSNP(FITC)-SS-PNA(−), demonstrating that the efficacy of delivered antisense PNA(Bcl-2) is sequence-specific (Figure S11a in the SI). To rule out the possibility of toxic effect that might lead to low protein expression, the cytotoxicities of free PNA(Bcl-2), MSNP(FITC)-SS-COOH, and MSNP(FITC)-SS-PNA(Bcl-2) were investigated by (3-(4,5-dimethylthiazol-2-yl)-2,5-diphenyltetrazolium bromide (MTT) assay. Low toxicity of the nanoparticles was observed under moderate concentrations (Figure S12 in the SI).[21] The cell toxicity does not result from the change of Bcl-2 gene expression, because the Bcl-2 protein level does not correlate with the cell viability. For HeLa cells treated with MSNP(FITC)-PNA(Bcl-2) without the disulfide bond linkage, the expression of Bcl-2 protein remained at a relatively high level, supporting that cleavable disulfide bond is important for controlled delivery of bioactive PNA inside HeLa cells (Figure S11b in the SI). We did not observe any protein silencing by using free PNA(Bcl-2) (Figure 11c in the SI), which might be attributed to low cellular uptake of free PNA (Figure S10 in the SI). In another control experiment, a control PNA PNA(Bcl-2 mm) was synthesized, which may form a destabilized duplex with bcl-2 mRNA with two mismatches (Table 1). PNA(Bcl-2 mm) was conjugated onto MSNP(FITC) via the disulfide linkage, designated as MSNP(FITC)-SS-PNA(Bcl-2 mm). However, no obvious gene silencing effect was observed by using MSNP(FITC)-SS-PNA(Bcl-2 mm), indicating the high sequence specificity of the PNA(Bcl-2) sequence against Bcl-2 protein expression (Figure 11d in the SI). Taken together, our results suggest that the delivery and controlled release of bioactive PNAs can be facilitated by the MSNP-PNA conjugates. Optimization of the functionalization of the MSNP and the conjugation chemistry with PNA may further improve the potency and reduce the toxicity.

CONCLUSION

In summary, we have successfully conjugated 18-mer antisense PNA sequences onto the MSNP(FITC) surface. After intracellular internalization, PNA(Bcl-2) has been delivered into the cytoplasm of HeLa cells in a redox-controlled release manner. High silencing efficacy of delivered PNA(Bcl-2) for the Bcl-2 protein expression in HeLa cells has been semiquantified by the Western blot assay. The present work may provide the foundation for further developments of combined gene therapy and chemotherapy in the treatment of certain cancers with overexpression of Bcl-2 protein.

EXPERIMENTAL SECTION

Materials. Absolute EtOH (>99.9%), acetic acid, β-actin primary antibody (Rabbit), and secondary antibody (goat anti-mouse and goat anti-rabbit), *aeg*PNA monomers, 2-aminoethylthiolhydrochloride, 3-aminopropyltriethoxysilane (APTES), Bcl-2 primary antibody (Mouse), bovine serum albumin (BSA), cetyltrimethylammonoium bromide (CTAB, 90%), Cy5 azide dye, 4′,6-diamidino-2-phenylindole (DAPI), diethyl ether, dimethylformamide (DMF, 99%), (3-(4,5-dimethylthiazol-2-yl)-2,5-diphenyltetrazolium bromide (MTT), 2,2′-dithiodipyridine, dithiothreitol (DTT), Dulbecco's modified Eagle's medium (DMEM), 1-ethyl-3-(3-(dimethylamino)propyl)carbodiimide (EDC), fetal bovine serum (FBS), fluorescein isothiocyanate (FITC), hydrochloride (HCl, assay 37%), 3-*N*-hydroxylsuccinimide (NHS), lysis buffer, LysoTracker, mercaptopyl trimethoxysilane (MPTMS), methanol (MeOH, 99.5%), Pierce BCA protein assay kit, phosphate buffered saline (PBS, pH 7.2) buffer, sodium

dx.doi.org/10.1021/bc5002714 | *Bioconjugate Chem.* 2014, 25, 1412−1420

Scheme 2. Chemical Structures of PNA Oligomers and Their Conjugates

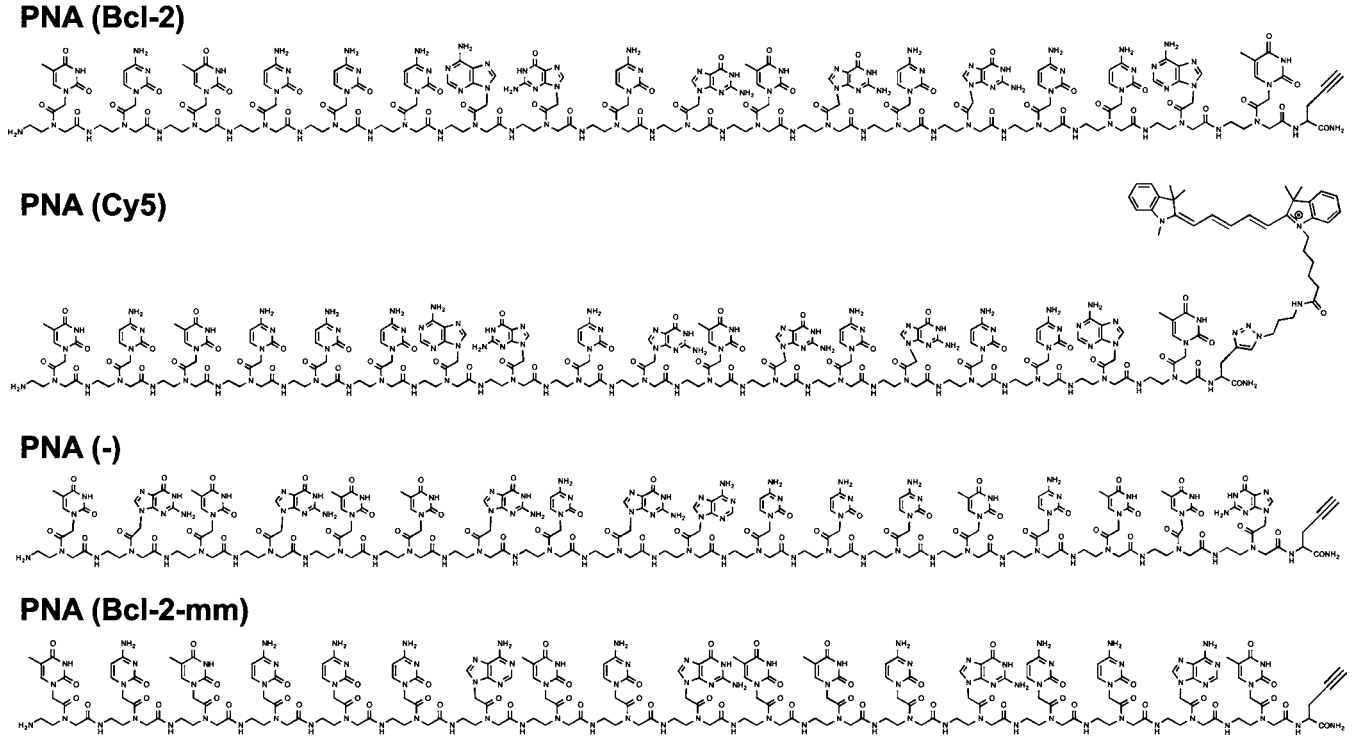

hydroxide (NaOH), succinic anhydride, tetraethylorthosilicate (TEOS, 99%), and thiopyridyldisulfide were purchased commercially.

Instruments. TEM images were captured by JEOL 2010 TEM at 200 kV, and FE-SEM images were taken by JEOL FESEM 6340 at 5 kV. Powder X-ray diffraction patterns were collected by X'Pert XRD. Zeta potential values were measured by Mavern Nanosizer. N_2 adsorption/desorption measurements were performed by ASAP 2020 Micromeritics. FT-IR spectra were collected through Fourier transformed infrared spectrometer. Fluorescence spectra were collected by RF-5301 spectrofluorophotometer. UV−vis spectra were measured by UV−vis 2501 spectrometer. A microplate reader (infinite 200 PRO, Tecan) was used for the MTT assay. Confocal microscopy images were taken by a confocal microscope (Leica TCS SP5, 40× oil objective). Western blot assay was completed with Invitrogen's Western Blotting Kits.

Synthesis of PNA Oligomers. The PNA oligomers were synthesized by solid phase peptide synthesis method from 4-methylbenzhydrylamine hydrochloride (MBHA·HCl) polystyrene based resin.[27] The resin has a reduced loading value of 0.35 mmol g^{-1}. The reduction of the loading value was carried out using acetic anhydride. (Benzotriazol-1-yloxy) tripyrrolidinophosphonium hexafluorophosphate/*N*,*N*-diisopropylethylamine (PyBOP/DIPEA) was used as the coupling reagent. Boc protection strategy was used during the oligomer synthesis. After sequential deprotection of *t*-Boc group and coupling of *aeg*PNA monomers on solid support, oligomers were cleaved from solid support by using "high-low trifluoroacetic acid-trifluoromethanesulfonic acid (TFA-TFMSA)" method. The oligomers were precipitated with diethyl ether, and subsequently dissolved in water, and purified by RP-HPLC using water-CH_3CN-0.1% trifluoroacetic acid (TFA) as the mobile phase. The matrix used for the characterization of the PNA oligomers by MALDI-TOF MS was α-cyano-4-hydroxycinnamic acid (CHCA).

Fluorescent Dye Cy5 Labeled PNA (PNA(Cy5)). To a solution of PNA (169.1 μM, 1 equiv) dissolved in DMSO (200 μL) and triethylammonium acetate (TEAA) buffer (2 M, pH 7.0, 100 μL), Cy5 azide (253.7 μM, 1.5 equiv) from a stock of DMSO solution (10 mM) was added. The solution was thoroughly mixed followed by the addition of freshly prepared ascorbic acid aqueous solution (0.5 mM). Degassing was carried out for the reaction mixture by bubbling nitrogen gas into it for 30 s. Required amount of $CuSO_4{\cdot}5H_2O$ (0.5 mM) from a stock of freshly prepared $CuSO_4{\cdot}5H_2O$ aqueous solution (10 mM) was added to the above reaction mixture. The final volume of the reaction mixture was adjusted to 500 μL with TEAA buffer (2 M). The reaction mixture was then flushed with nitrogen gas and left in a rotator at room temperature overnight. The purification and characterization of the dye-conjugated product were carried out by RP-HPLC and MALDI-TOF MS, respectively. The chemical structures of the PNAs are shown in Scheme 2.

Synthesis of MSNP(FITC). FITC labeled MSNP, i.e., MSNP(FITC), was synthesized by a co-condensation method.[17,21] In a typical synthesis, CTAB (500 mg) was dissolved in deionized H_2O (250 mL). NaOH aqueous solution (1.75 mL, 2 M) was added into the above solution. The mixture solution was heated to 80 °C under vigorous stirring. Meanwhile, FITC (1.3 mg) was dissolved in absolute ethanol (1.5 mL) and mixed with APTES (3 μL) in the dark for 2 h before adding into TEOS (2.5 mL). When temperature of the CTAB solution was stabilized at 80 °C, the TEOS (2.5 mL) solution containing FITC was slowly added into the solution, which was kept under stirring at 80 °C for 2 h. The formed nanoparticles, MSNP(FITC), were collected by centrifugation at 8000 rpm for 10 min and washed with MeOH and deionized water. The nanoparticles were dried in vacuo at 80 °C for 24 h.

dx.doi.org/10.1021/bc5002714 | *Bioconjugate Chem.* 2014, 25, 1412−1420

Synthesis of Solid Silica Nanoparticles (Solid SiO_2). Typically, ethanol (142.8 mL), deionized water (20 mL), and ammonium aqueous solution (25−28%, 4 mL) were mixed under stirring. After the mixture solution was heated to 30 °C, TEOS (6 mL) was added to the mixture. The reaction mixture was stirred at 30 °C for 6 h. The formed solid SiO_2 nanoparticles were collected by centrifugation and washed with deionized water and ethanol thoroughly.

Synthesis of MSNP(FITC)-SH and Solid SiO_2-SH. The introduction of thiol units through a grafting method was conducted by suspending MSNP(FITC) or solid SiO_2(500 mg) in MeOH (50 mL), followed by the addition of MPTMS (0.5 mL). The mixture solution was refluxed at 80 °C under N_2 atmosphere for 24 h. The thiol group functionalized silica nanoparticles, MSNP(FITC)-SH and solid SiO_2-SH, were collected by centrifugation and washed with MeOH and deionized H_2O. Surfactant was removed by suspending MSNP(FITC)-SH in MeOH (50 mL) containing condensed HCl (3 mL, 37%) and refluxing at 80 °C for 24 h. Porous MSNP(FITC)-SH was collected by centrifugation and washed thoroughly with MeOH and deionized H_2O. Finally, porous MSNP(FITC)-SH and solid SiO_2-SH were dried in vacuo at 80 °C for 24 h before the characterizations.

Synthesis of *S*-(2-Aminoethylthio)-2-thiopyridine Hydrochloride. The compound was prepared according to a previous literature report.[28] Typically, thiopyridyldisulfide (4.4 g) was dissolved in MeOH (20 mL), and acetic acid (0.8 mL) was then added. MeOH solution (10 mL) containing 2-aminoethylthiolhydrochloride (1.1 g) was dropwise added into the above solution within 30 min. After the mixture solution was stirred for 48 h, the solvent was removed in vacuo, leading to a yellow oil product. The oil was washed with diethyl ether (50 mL) and then dissolved in MeOH (10 mL). The product was precipitated by the addition of diethyl ether (200 mL), chilled at −20 °C for 24 h, and collected by filtration in vacuo. The product was reprecipitated in MeOH (10 mL) in order to afford a pure compound.

Synthesis of MSNP(FITC)-SS-NH_2 and Solid SiO_2-SS-NH_2. MSNP(FITC)-SH or solid SiO_2-SH (200 mg) was suspended in MeOH (30 mL), and then *S*-(2-aminoethylthio)-2-thiopyridine hydrochloride (200 mg) was added. The mixture solution was stirred at room temperature for 24 h to yield MSNP(FITC)-SS-NH_2 or solid SiO_2-SS-NH_2. The nanoparticles were collected by centrifugation, washed thoroughly with MeOH and deionized H_2O, and dried under vacuo at 80 °C for 24 h.

Determination of −SS-NH_2 Group Amount on Nanoparticles. The synthesized nanoparticles, MSNP(FITC)-SS-NH_2 and solid SiO_2-SS-NH_2, were fully suspended in MeOH (1 mg mL^{-1}). Then, each nanoparticle suspension (20 μL) was added into MeOH solution (1 mL) containing fluorescamine (20 μg mL^{-1}). After 30 min incubation, the fluorescence intensity (475 nm) of the mixture was measured by excitation at 375 nm. A MeOH solution containing known concentrations of APTES was used as standard to quantify the concentration of primary amine group.

Synthesis of MSNP(FITC)-NH_2. MSNP(FITC) (500 mg) was suspended in ethanol (25 mL), and APTES (0.5 mL) was added into the solution. The mixture solution was stirred at room temperature for 48 h. The amine-modified nanoparticles were collected by centrifugation and washed by MeOH and deionized H_2O. Then, the collected nanoparticles were suspended in MeOH (50 mL) containing condensed HCl (3 mL, 37%) and kept refluxing at 80 °C for 24 h in order to remove the surfactant CTAB. Obtained MSNP(FITC)-NH_2 was collected by centrifugation and washed thoroughly with MeOH and deionized H_2O. MSNP(FITC)-NH_2 was dried in vacuo at 80 °C for 24 h before the characterizations.

Synthesis of MSNP(FITC)-SS-COOH and MSNP(FITC)-COOH. MSNP(FITC)-SS-NH_2 or MSNP(FITC)-NH_2 (200 mg) was suspended in DMF containing succinic anhydride (1.2 g) and TEA (1.3 mL). The mixture solution was stirred for 24 h. The nanoparticles were collected by centrifugation and thoroughly washed by DMF and MeOH. Then, obtained MSNP(FITC)-SS-COOH or MSNP(FITC)-COOH was dried in vacuo at 80 °C for 24 h before further characterization or PNA conjugation.

MSNP-PNA Conjugation. MSNP(FITC)-SS-COOH or MSNP(FITC)-COOH (1 mg, 1 equiv) was used for the conjugation with PNA(Bcl-2), PNA(Cy5), PNA(−), and PNA(Bcl-2 mm). EDC (22 mg, 500 equiv) and NHS (11 mg, 500 equiv) were added to MSNP(FITC)-SS-COOH or MSNP(FITC)-COOH aqueous suspension to activate the carboxylic acid units. Reaction mixture was incubated at room temperature for 15 min followed by the addition of Cy5 dye labeled (5% of MSNP weight) or unlabeled PNA (20% of MSNP weight). A rotator was used to ensure continuous mixing of the reaction mixture at room temperature. After overnight incubation, the reaction mixture was centrifuged at 10 000 rpm for 5 min. Upon removal of the supernatant, the conjugated nanoparticles were thoroughly washed (1 mL × 8) by RNase free water. PNA conjugated nanoparticles (MSNP-(FITC)-SS-PNA(Bcl-2), MSNP(FITC)-SS-PNA(Cy5), MSNP(FITC)-SS-PNA(−), MSNP(FITC)-SS-PNA(Bcl-2 mm), MSNP(FITC)-PNA(Bcl-2), MSNP(FITC)-PNA(Cy5), and MSNP(FITC)-PNA(−) were stored at 4 °C.

PNA(Cy5) Release Test. MSNP(FITC)-SS-PNA(Cy5) (1 mg) was suspended in PBS buffer (1 mL, pH 7.2) without or with DTT (10 mM and 20 mM). The suspension was incubated for certain time interval before centrifugation at 13 000 rpm for 3 min. The Cy5 fluorescence intensity (655 nm) of the supernatant was recorded in order to trace the PNA(Cy5) release process. After the release test, excess DTT was added into the suspension to completely release all PNA(Cy5). Then, the suspension was centrifuged, and the total PNA(Cy5) amount that was conjugated onto MSNP(FITC) was quantified by comparing the Cy5 fluorescence intensity of the supernatant at 655 nm with a standard sample.

MTT Cytotoxicity Assay. The cytotoxicity of free PNA, MSNP(FITC)-SS-COOH, and MSNP(FITC)-SS-PNA(Bcl-2) was evaluated by MTT assay. HeLa cells were seeded into 96-well plate at a density of 1×10^4 cells/well in DMEM medium. After 24 h incubation, the medium in the wells was replaced with fresh medium (100 μL) containing various concentrations of free PNA, MSNP(FITC)-SS-COOH, and MSNP(FITC)-SS-PNA(Bcl-2). After incubation for another 24 h, the medium was replaced by fresh medium and then cells were further cultured for 48 h before the MTT assay. For the MTT assay, old medium was removed and new medium (100 μL) containing MTT (0.5 mg mL^{-1}) was added into each well. After incubation for 4 h, the medium was replaced with DMSO (100 μL). The plate was gently shaken for 15 min before measuring the absorbance at 565 nm by using a microplate reader. The cell viability related to the control wells that only contain cell culture medium was calculated by $[A]_{test}/[A]_{control}$,

dx.doi.org/10.1021/bc5002714 | *Bioconjugate Chem.* 2014, 25, 1412−1420

where $[A]_{test}$ and $[A]_{control}$ are the average absorption intensities of the test and control samples, respectively.

Confocal Laser Scanning Microscopy (CLSM) Images. HeLa cells were seeded in plastic confocal dishes (35 mm) and grown in DMEM medium for 24 h. Then, the medium was changed into new medium containing MSNP(FITC)-SS-PNA(Cy5) (20 μg mL^{-1}), MSNP(FITC)-PNA(Cy5) (20 μg mL^{-1}), or Free PNA(Cy5) (1 μM). After incubation for required time intervals, the medium was removed and the cells were washed three times by PBS. Then, the cells were fixed with 4.0% formaldehyde at room temperature for 15 min. After washing with PBS, the cells were stained with DAPI (0.025 μg mL^{-1}) for 15 min. Finally, the cells were washed by PBS before the CLSM observation.

Bcl-2 Protein Expression Knockdown and Western Blot Assay. HeLa cells were seeded into 6-well plate at a density of 20×10^4 cells/well in complete DMEM medium and grown for 24 h. Then, the medium was replaced by new medium containing MSNP(FITC)-SS-PNA(Bcl-2) at different concentrations. For the negative control groups, HeLa cells were treated with MSNP(FITC)-SS-PNA(−), MSNP(FITC)-PNA(Bcl-2), free PNA(Bcl-2), or MSNP(FITC)-SS-PNA(Bcl-2 mm) at various concentrations. HeLa cells without any treatment were used as a control in each group. After 24 h incubation, the medium in each well was replaced by new medium and the cells were further incubated for 48 h. Three independent experiments were carried out for the statistic evaluation. For the protein collection, the culture medium was removed and the cells were washed with chilled PBS buffer (pH 7.2) three times. After adding lysis buffer (250 μL), the plate was shaken at 4 °C for 30 min in order to break cell membranes. The lysis buffer was collected and centrifuged (13 000 rpm, 4 °C) for 10 min, and the supernatant was then collected. Proteins collected from HeLa cells without any treatment during the whole process were used as controls. The protein concentration was quantified by Pierce BCA Protein Assay Kit according to its product instruction to ensure that there were equal amount of proteins loaded inside each well during the Western blot assay. Relative Bcl-2 protein expression level was checked by Western blot assay using β-actin as an internal standard, which was carried out according to its standard protocol. Relative protein expression level was normalized by comparing the band intensity to that of the control group in the Western blot assay. After obtaining the Western blot bands, the Bcl-2 band intensity and corresponding β-actin band intensity were read by using software ImageJ. The ratio of Bcl-2 band intensity to that of β-actin was calculated. The ratio of the control group without any treatment was taken as 100%, and the calculated ratios were normalized to the percentage values according to the control group.

■ ASSOCIATED CONTENT

Supporting Information

Additional characterization figures, spectra, and data. This material is available free of charge via the Internet at http://pubs.acs.org.

■ AUTHOR INFORMATION

Corresponding Authors

*E-mail: rnachen@ntu.edu.sg.

*E-mail: zhaoyanli@ntu.edu.sg.

Author Contributions

Xing Ma and Gitali Devi contributed equally to this work.

Notes

The authors declare no competing financial interest.

■ ACKNOWLEDGMENTS

This research project is supported by the National Research Foundation (NRF), Prime Minister's Office, Singapore under its NRF Fellowship (NRF2009NRF-RF001-015 to Y.Z.), Campus for Research Excellence and Technological Enterprise (CREATE) Programme (to Y.Z.), the NTU-A*Star Centre of Excellence for Silicon Technologies (A*Star SERC No.: 112 351 0003 to Y.Z.), as well as Singapore Ministry of Education (MOE) Tier 1 (RGT3/13 to G.C.) and MOE Tier 2 (MOE2013-T2-2-024 to G.C.).

■ REFERENCES

(1) Adams, J. M., and Cory, S. (1998) The Bcl-2 protein family: arbiters of cell survival. *Science 281*, 1322−1326.

(2) Youle, R. J., and Strasser, A. (2008) The BCL-2 protein family: opposing activities that mediate cell death. *Nat. Rev. Mol. Cell Biol. 9*, 47−59.

(3) Chen, A. M., Zhang, M., Wei, D. G., Stueber, D., Taratula, O., Minko, T., and He, H. X. (2009) Co-delivery of doxorubicin and Bcl-2 siRNA by mesoporous silica nanoparticles enhances the efficacy of chemotherapy in multidrug-resistant cancer cells. *Small 5*, 2673−2677.

(4) Saad, M., Garbuzenko, O. B., and Minko, T. (2008) Co-delivery of siRNA and an anticancer drug for treatment of multidrug-resistant cancer. *Nanomedicine 3*, 761−776.

(5) Wang, Y., Gao, S., Ye, W.-H., Yoon, H. S., and Yang, Y.-Y. (2006) Co-delivery of drugs and DNA from cationic core-shell nanoparticles self-assembled from a biodegradable copolymer. *Nat. Mater. 5*, 791−796.

(6) Egholm, M., Buchardt, O., Christensen, L., Behrens, C., Freier, S. M., Driver, D. A., Berg, R. H., Kim, S. K., Norden, B., and Nielsen, P. E. (1993) PNA hybridizes to complementary oligonucleotides obeying the Watson−Crick hydrogen-bonding rules. *Nature 365*, 566−568.

(7) Nielsen, P. E., Egholm, M., Berg, R., and Buchardt, O. (1991) Sequence-selective recognition of DNA by strand displacement with a thymine-substituted polyamide. *Science 254*, 1497−1500.

(8) Sethi, D., Chen, C.-P., Jing, R.-Y., Thakur, M. L., and Wickstrom, E. (2012) Fluorescent peptide−PNA chimeras for imaging monoamine oxidase a mRNA in neuronal cells. *Bioconjugate Chem. 23*, 158−163.

(9) Good, L., and Nielsen, P. E. (1998) Antisense inhibition of gene expression in bacteria by PNA targeted to mRNA. *Nat. Biotechnol. 16*, 355−358.

(10) Shiraishi, T., and Nielsen, P. E. (2011) Improved cellular uptake of antisense peptide nucleic acids by conjugation to a cell-penetrating peptide and a lipid domain, in *Bioconjugation Protocols* (Mark, S. S., Ed.) pp 209−221, Humana Press, Totowa, NJ.

(11) Gallazzi, F., Wang, Y., Jia, F., Shenoy, N., Landon, L. A., Hannink, M., Lever, S. Z., and Lewis, M. R. (2003) Synthesis of radiometal-labeled and fluorescent cell-permeating peptide−PNA conjugates for targeting the Bcl-2 proto-oncogene. *Bioconjugate Chem. 14*, 1083−1095.

(12) Koppelhus, U., and Nielsen, P. E. (2003) Cellular delivery of peptide nucleic acid (PNA). *Adv. Drug Delivery Rev. 55*, 267−280.

(13) Duy, J., Connell, L., Eck, W., Collins, S., and Smith, R. (2010) Preparation of surfactant-stabilized gold nanoparticle−peptide nucleic acid conjugates. *J. Nanopart. Res. 12*, 2363−2369.

(14) Saleh, A. F., Arzumanov, A., Abes, R., Owen, D., Lebleu, B., and Gait, M. J. (2010) Synthesis and splice-redirecting activity of branched, arginine-rich peptide dendrimer conjugates of peptide nucleic acid oligonucleotides. *Bioconjugate Chem. 21*, 1902−1911.

(15) Slowing, I. I., Vivero-Escoto, J. L., Wu, C. W., and Lin, V. S. Y. (2008) Mesoporous silica nanoparticles as controlled release drug

delivery and gene transfection carriers. *Adv. Drug Delivery Rev. 60*, 1278−1288.
(16) Ashley, C. E., Carnes, E. C., Epler, K. E., Padilla, D. P., Phillips, G. K., Castillo, R. E., Wilkinson, D. C., Wilkinson, B. S., Burgard, C. A., Kalinich, R. M., Townson, J. L., Chackerian, B., Willman, C. L., Peabody, D. S., Wharton, W., and Brinker, C. J. (2012) Delivery of small interfering RNA by peptide-targeted mesoporous silica nanoparticle-supported lipid bilayers. *ACS Nano 6*, 2174−2188.
(17) Zhang, Q., Liu, F., Nguyen, K. T., Ma, X., Wang, X. J., Xing, B. G., and Zhao, Y. L. (2012) Multifunctional mesoporous silica nanoparticles for cancer-targeted and controlled drug delivery. *Adv. Funct. Mater. 22*, 5144−5156.
(18) Cheng, R., Feng, F., Meng, F., Deng, C., Feijen, J., and Zhong, Z. (2011) Glutathione-responsive nano-vehicles as a promising platform for targeted intracellular drug and gene delivery. *J. Controlled Release 152*, 2−12.
(19) Luo, Z., Cai, K. Y., Hu, Y., Li, J. H., Ding, X. W., Zhang, B. L., Xu, D. W., Yang, W. H., and Liu, P. (2012) Redox-responsive molecular nanoreservoirs for controlled intracellular anticancer drug delivery based on magnetic nanoparticles. *Adv. Mater. 24*, 431−435.
(20) Webb, A., Cunningham, D., Cotter, F., Clarke, P. A., Di Stefano, F., Ross, P., Corbo, M., and Dziewanowska, Z. (1997) Bcl-2 antisense therapy in patients with non-Hodgkin lymphoma. *Lancet 349*, 1137−1141.
(21) Ma, X., Nguyen, K. T., Borah, P., Ang, C. Y., and Zhao, Y. (2012) Functional silica nanoparticles for redox-triggered drug/ssDNA co-delivery. *Adv. Healthcare Mater. 1*, 690−697.
(22) Stöber, W., Fink, A., and Bohn, E. (1968) Controlled growth of monodisperse silica spheres in the micron size range. *J. Colloid Interface Sci. 26*, 62−69.
(23) Rostovtsev, V. V., Green, L. G., Fokin, V. V., and Sharpless, K. B. (2002) A stepwise Huisgen cycloaddition process: copper(I)-catalyzed regioselective "ligation" of azides and terminal alkynes. *Angew. Chem., Int. Ed. 41*, 2596−2599.
(24) Lewis, M. R., Jia, F., Gallazzi, F., Wang, Y., Zhang, J., Shenoy, N., Lever, S. Z., and Hannink, M. (2002) Radiometal-labeled peptide−PNA conjugates for targeting Bcl-2 expression: preparation, characterization, and in vitro mRNA binding. *Bioconjugate Chem. 13*, 1176−1180.
(25) Voehringer, D. W., McConkey, D. J., McDonnell, T. J., Brisbay, S., and Meyn, R. E. (1998) Bcl-2 expression causes redistribution of glutathione to the nucleus. *Proc. Natl. Acad. Sci. U.S.A. 95*, 2956−2960.
(26) Koppelhus, U., Shiraishi, T., Zachar, V., Pankratova, S., and Nielsen, P. E. (2008) Improved cellular activity of antisense peptide nucleic acids by conjugation to a cationic peptide-lipid (CatLip) domain. *Bioconjugate Chem. 19*, 1526−1534.
(27) Devi, G., Yuan, Z., Lu, Y., Zhao, Y., and Chen, G. (2014) Incorporation of thio-pseudoisocytosine into triplex-forming peptide nucleic acids for enhanced recognition of RNA duplexes. *Nucleic Acids Res. 42*, 4008−4018.
(28) Ebright, Y. W., Chen, Y., Kim, Y., and Ebright, R. H. (1996) *S*-[2-(4-Azidosalicylamido)ethylthio]-2-thiopyridine: radioiodinatable, cleavable, photoactivatible cross-linking agent. *Bioconjugate Chem. 7*, 380−384.